NASA Technical Memorandum 84606

NASA-TM-84606 19830009628

STRUCTURAL TESTING FOR
STATIC FAILURE, FLUTTER
AND OTHER SCARY THINGS

RODNEY H. RICKETTS

JANUARY 1983

NASA

National Aeronautics and
Space Administration

Langley Research Center
Hampton, Virginia 23665

STRUCTURAL TESTING FOR STATIC FAILURE, FLUTTER AND OTHER SCARY THINGS

Rodney H. Ricketts

SUMMARY

Ground test and flight test methods are described that may be used to highlight potential structural problems that occur on aircraft. Primary interest is focused on light-weight general aviation airplanes. The structural problems described include static strength failure, aileron reversal, static divergence, and flutter. An example of each of the problems is discussed to illustrate how the data acquired during the tests may be used to predict the occurrence of the structural problem. While this report gives some rules of thumb for the prediction of structural problems, it is not intended to be used explicitly as a structural analysis handbook. However, many such handbooks are included in the reference list.

INTRODUCTION

All aircraft have inherent structural flexibilities that may contribute to the cause of many types of problems--some destructive in nature. These flexibilities may couple with aerodynamic forces or with inertia forces to produce unwanted structural instabilities. To insure that these structural problems do not occur within the flight envelope, it is necessary to perform certain tests and/or analyses on the aircraft. A typical structural integrity verification program for a commercial aircraft includes the following elements: (1) extensive design-cycle analyses which may use computer simulations (called finite element models) to predict the response of the aircraft; (2) ground tests of the fabricated parts, both in the unassembled state and assembled to form the complete aircraft; (3) more analyses using the data acquired during the ground test to verify or calibrate the analytical results; (4) wind-tunnel tests of models which simulate the full scale article; and, finally (5) flight test of the completed aircraft throughout the flight envelope. Performing these tasks provides the safest means for verifying that the aircraft structure will hold together during operation.

This paper focuses on two of the above elements--namely, ground test and flight test techniques that may be used to predict the occurrence of potential structural problems. While methods are described herein that are applicable to all classes of aircraft, emphasis is placed on simple and inexpensive methods that may be used by individuals who are building their own general-aviation-class airplane. The problems that are discussed include static strength failure, aileron reversal, static divergence, and flutter. For each of these problems the following is given: a description of the problem; procedures for structural testing for the problem and an explanation of the use of the results; requirements set forth in the Federal Aviation Regulations as standards for airworthiness of the aircraft experiencing the problem; and an example of an application of the procedures used at the National Aeronautics and Space Administration (NASA) in ground, wind-tunnel, or flight tests. While this report gives some rules of thumb for the prediction of structural problems, it is not intended to be used explicitly as a structural analysis handbook. A more thorough discussion of these problems may be found in such books as references 1-3.
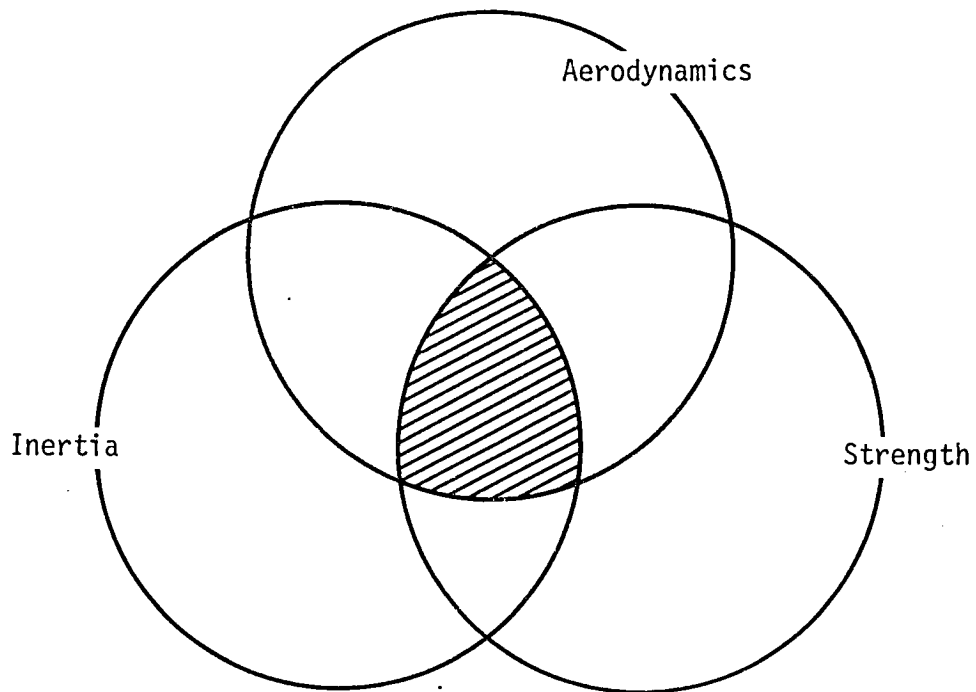
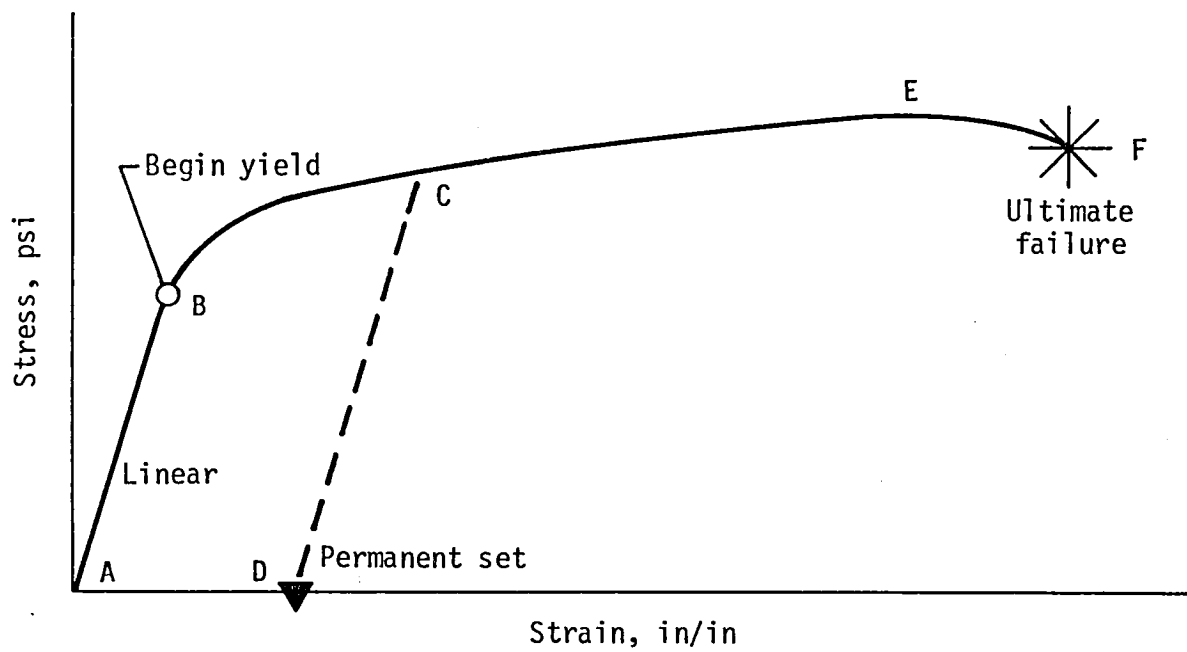Figure 1.- Interaction diagram for static strength failure.

Figure 2.- Stress-strain diagram for a typical metal.

STATIC STRENGTH FAILURE[1]

Static strength failure is the interaction of aerodynamics, inertia, and strength. The interaction diagram shown in figure 1 illustrates the interaction by the shaded area. It is the condition where the aerodynamic and inertia loads cause the structural stress to exceed the structural strength. At this condition the structure fails and is no longer capable of carrying the load. A failure can lead to catastrophic destruction of the aircraft.

A stress-strain curve for a typical metal is shown in figure 2. The curve shows three regions of interest. A region of linearity exists (segment AB) where the stress (related to applied load) is directly proportional to the strain (related to deformation) produced within the metal. When loaded and then unloaded within this region, the metal will return to a zero-strain (undeformed) condition. A region of non-linearity exists (segment BE) where the material begins to yield (or permanently stretch) under additional load. Metal loaded into the yield region (point C) and then unloaded will return along line CD which is parallel to the original linear region line to a deformed condition--one with a permanent set (point D). In this case, the linear region is shifted to the right, and the metal will respond along line DC when it is reloaded to point C. A region of failure exists (segment EF) where the ultimate strength of the metal is reached. The metal stretches rapidly to relieve the load and then fails at point F. Additional information is contained in reference 4.

---

[1]The figures and text in this paper are presented in the following format. All figures appear on left-hand pages (even numbers). The text describing each figure appears aligned to that figure on the opposing right-hand page (odd number).
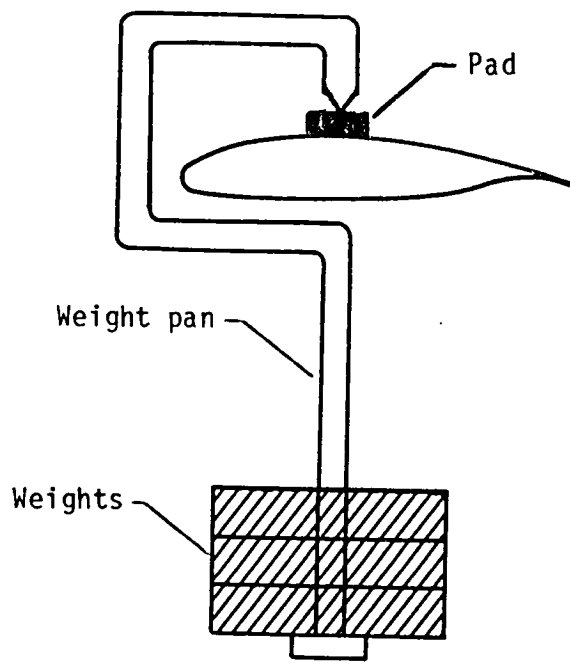
(a) Weight pan
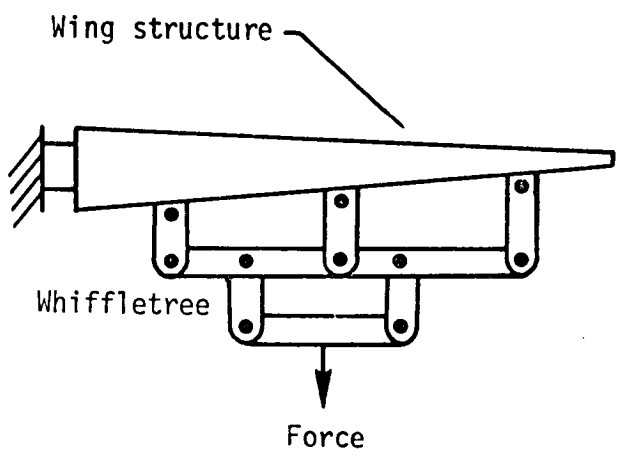
(b) Whiffletree

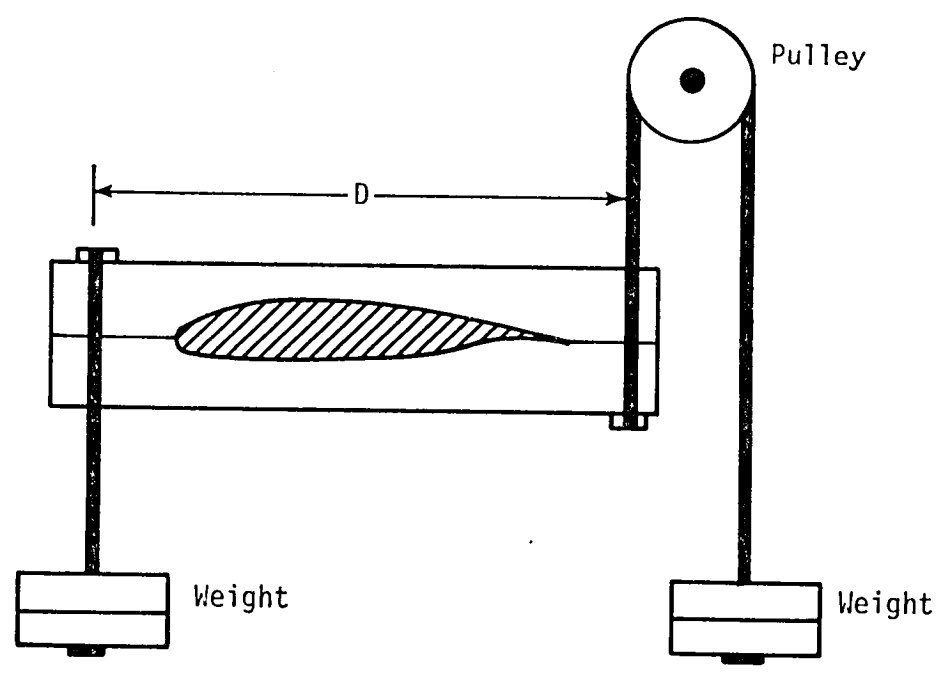Figure 3.- Two loading fixtures for applying forces.

Figure 4.- A typical loading fixture for applying moments.

During ground tests for static failure, loads in the form of forces and/or moments are applied to the structure, the stresses that are produced in the structure are measured, and the resulting structural deformations are measured. These procedures are discussed in the following text.

Forces may be applied to the structure as either point or distributed loads. For point forces a weight pan as shown in figure 3a may be used to support the weights as they are applied. A loading pad may be used so as not to puncture the structure with the pan fixture. Another method of applying point forces is through the use of a hydraulic ram. Distributed forces which represent an aerodynamic or inertia load condition may be applied by distributing sandbags or bags filled with lead shot across the structure. An alternate method for applying distributed loads is through a whiffletree apparatus which attaches to the structure at several points as shown in figure 3b. Forces then may be applied to the whiffletree using weights or a hydraulic ram.

A pure moment (couple) is produced when two equal loads are applied in opposite directions at different points on the structure. A torsional moment may be applied to a wing using two weight pans as shown in figure 4. One is attached to one end of a frame that snugly fits over the structure, while the other is attached to a cable routed over a pulley and connected to the other end of the frame. Equal weights are then applied to each weight pan. The moment is equivalent to the weight on either pan multiplied by the distance D between the attach points.
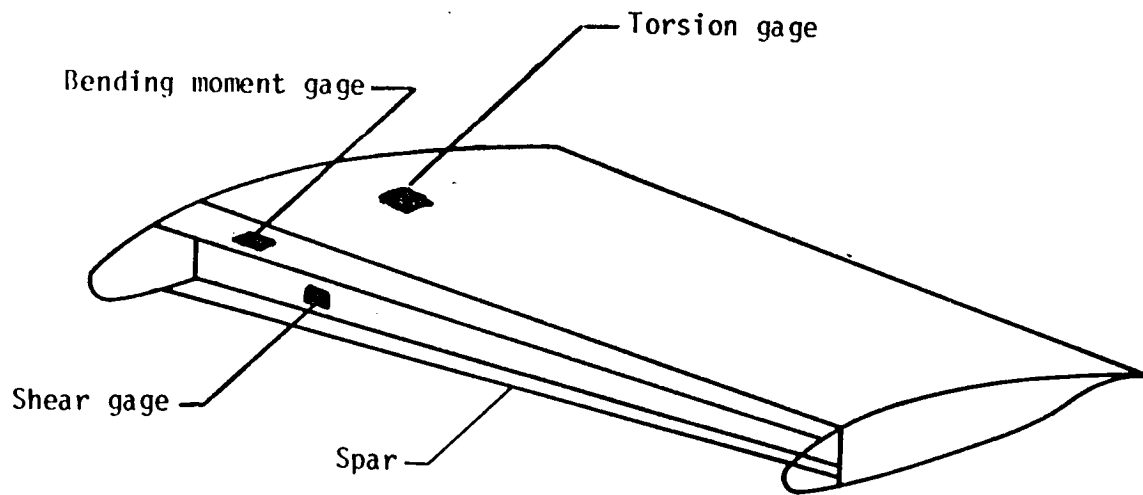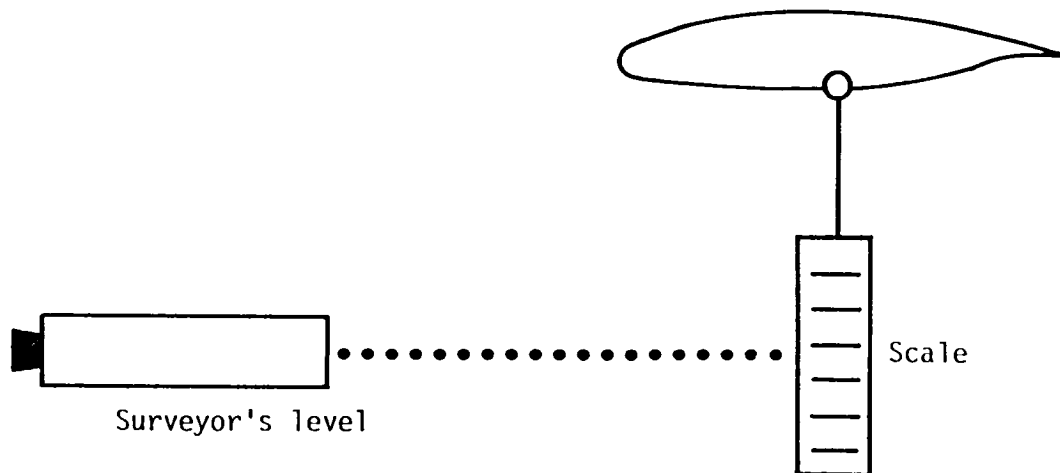
Figure 5.- Typical strain gage installation.

Figure 6.- A method for measuring displacements.

To measure the stress in a structure when it is loaded, small resistance wire gages connected in a Wheatstone bridge arrangement are used to measure the strain of the material. These strain gages, as they are called, are attached to the structure at specific locations, as shown in figure 5, and oriented in specific directions to measure such reactions as shear, bending moment, and torsion moment. Stress is proportional to strain in the linear range of the material. (See fig. 2.)

Structural deformations may be either linear (a displacement) or angular (a rotation) in nature. To measure a displacement a simple pointer attached to the structure and a scale attached to ground may be used. This method can give accuracy to 0.05 in. A slightly more accurate method requires a surveyor's level and a scale. The scale is hung from the structure and sighted with the level as shown in figure 6. This may give accuracy to 0.02 in. Mechanical dial gauges may be used to increase the accuracy of the measurements to 0.001 in.
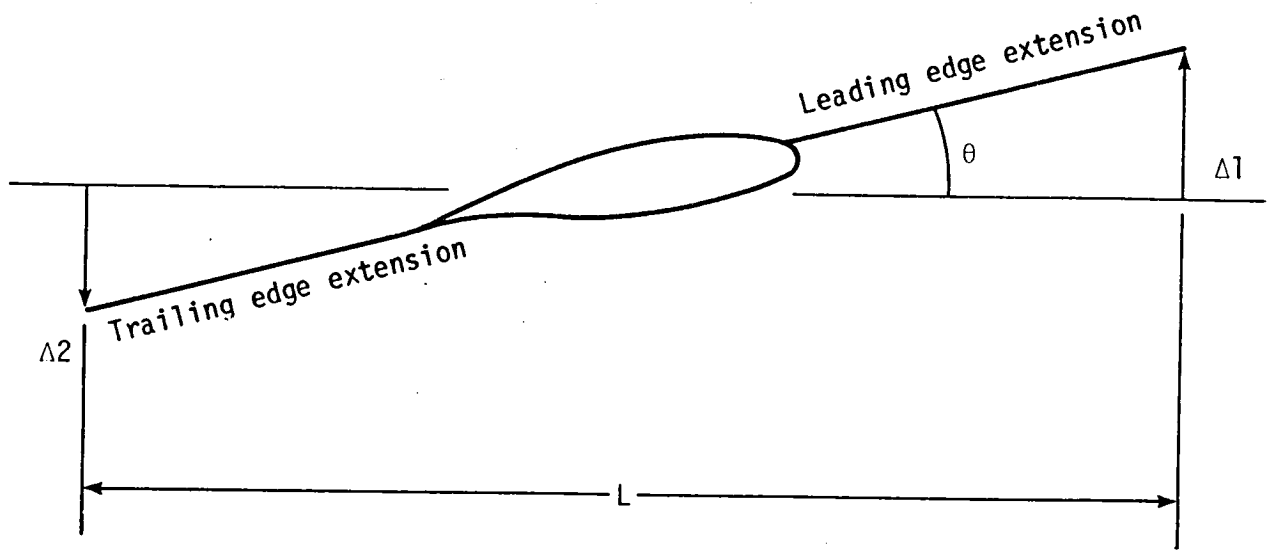
(a) Displacement method
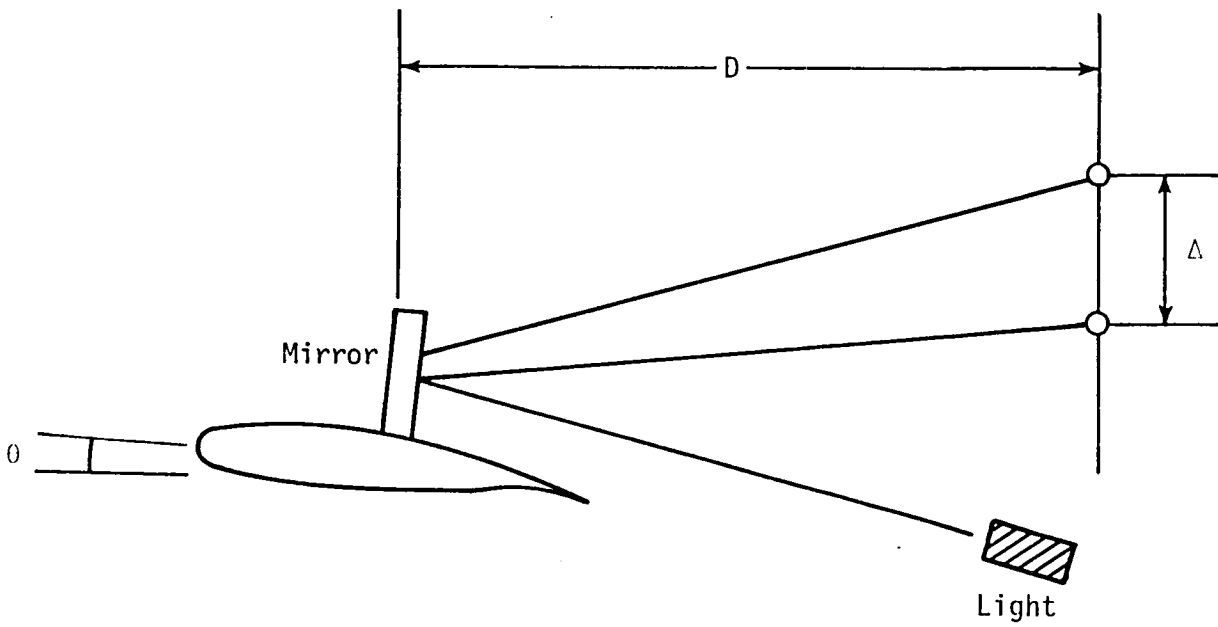
(b) Mirror method

Figure 7.- Two methods for measuring rotations.

Three methods are presented for measuring a rotation. The simplest involves displacement measurements at two points at a distance L apart on the structure as shown in figure 7a. For a small rotation, the angle θ is approximately equal to the tangent of the angle, or in other words, is equal to the sum of the displacements, $\Delta 1$ and $\Delta 2$, divided by the distance they are apart. That is,

$$\theta = (\Delta 1 + \Delta 2)/L.$$

Using another method which employs mirrors and a light source (a laser or simply a slide projector), rotation may be more accurately measured. The light is reflected by the mirror located on the structure to a wall some distance D away as shown in figure 7b. As the structure rotates, the light is deflected a distance Δ such that $\theta = \Delta/2D$. The third method for measuring rotation is through the use of an inclinometer, either a bubble-type or an electrical accelerometer-type.
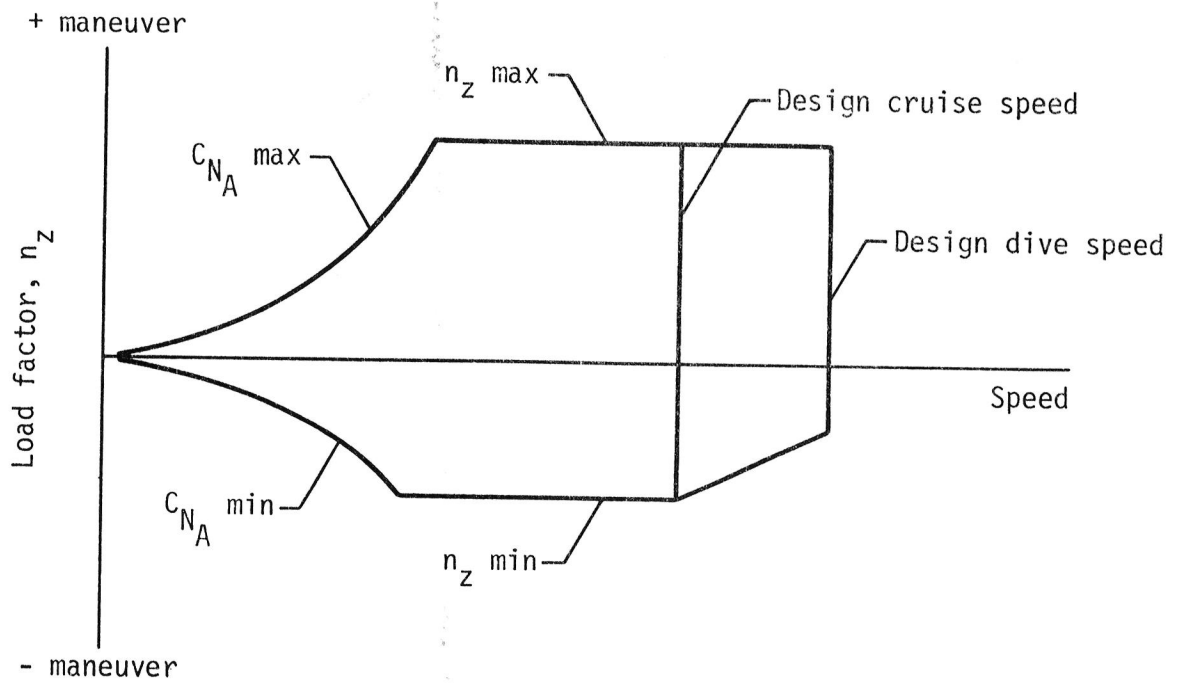
Figure 8.- Typical flight envelope in terms of speed and load factor.
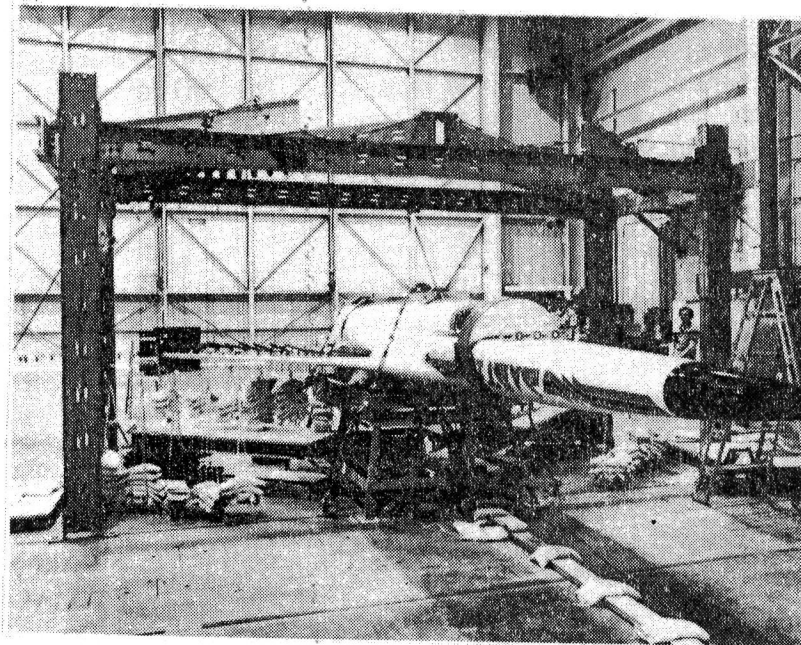

Figure 9.- Structural strength test of DAST flight vehicle.

10

The federal standards for airworthiness of normal, utility, and acrobatic category aircraft are presented in Federal Aviation Regulations, Part 23 (ref. 5). To be certified by the Federal Aviation Administration (FAA) an airplane must pass certain ground tests for static strength. The aircraft must be able to withstand the application of limit loads--that is, the maximum loads expected during service--without permanent or excessive deformations. A permanent deformtion may occur if the structure is loaded beyond the material yield point. In addition, the aircraft must withstand the application of ultimate loads--that is, a load 1.5 times as large as the limit load--for at least three seconds without failure.

The flight envelope defines the flight conditions for which the aircraft has been designed. This envelope can be defined in terms of speed and load factor as shown in figure 8. Load factor is the ratio of total aerodynamic lift to total airplane weight. The envelope is bounded by values of maximum and minimum normal lift coefficients C_{N_A} which may be reached during take-off and landing, by maximum and minimum load factors N_z which may occur during maneuvers, and by maximum airspeed conditions which may occur during cruise or dive. The limit loads defined for ground tests must be the maximum load conditions experienced within this flight envelope.

Figure 9 shows the setup for the structural loads test of the NASA Langley Research Center DAST (Drones for Aerodynamic and Structural Testing) flight-test vehicle. (See refs. 6 and 7.) The vehicle is supported upside down along the fuselage so that the wing structure is loaded for a positive maneuver condition. Many loading pan fixtures are attached to the front and rear spars. Shot bags are placed in specific pans to simulate a flight load condition.
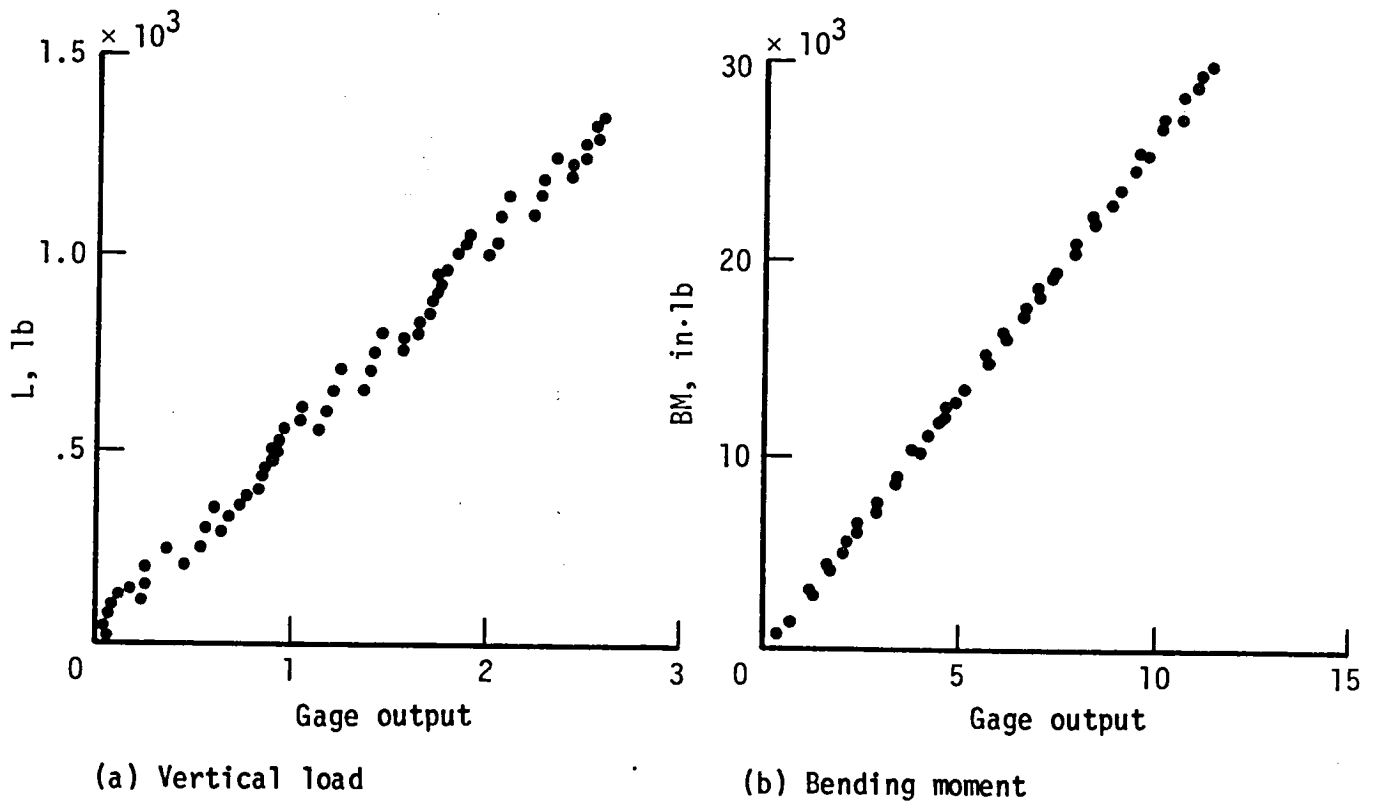
(a) Vertical load

(b) Bending moment

Figure 10.- Loads data measured on DAST flight vehicle.
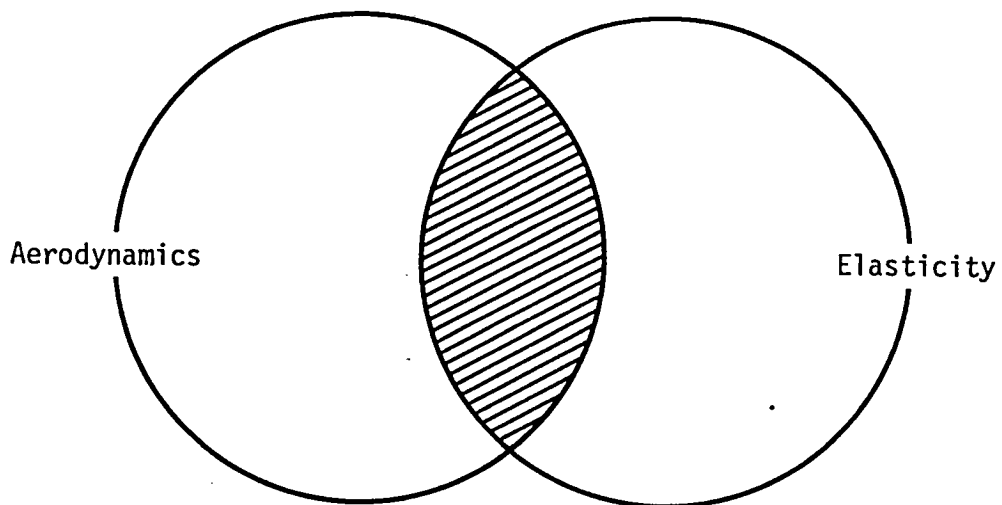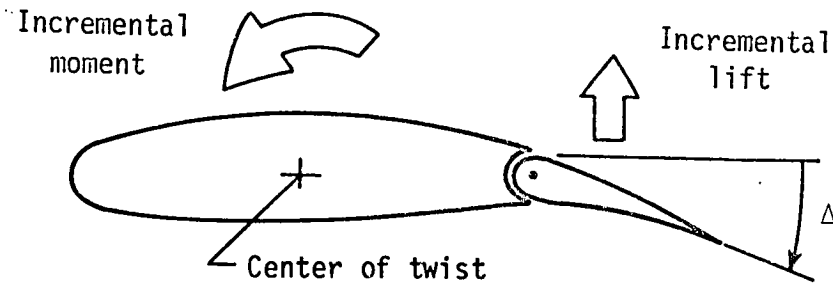

Aerodynamics

Elasticity

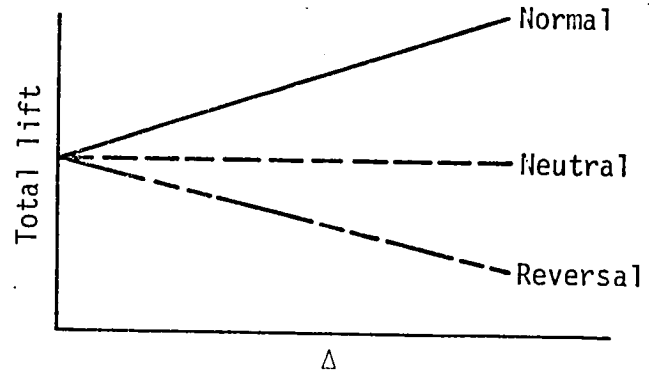Figure 11.- Interaction diagram for aileron reversal.

Data were acquired with strain gauges which were positioned to measure load L and bending moment BM. The data shown in figure 10 were acquired during the loading and unloading of many incremental loads. The data shown are linear (no yielding of the structure experienced) throughout the load range as is required.

- AILERON REVERSAL

Aileron reversal is the condition in which the control surface aerodynamic forces twists the wing in such a manner that a zero rolling moment exists. Any further increase in speed will cause the aircraft to roll opposite to the stick motion--that is, a stick right command will cause the aircraft to roll to the left. This phenomena is the interaction of aerodynamic and structural eleasticity as illustrated by the shaded area of figure 11.

Incremental moment

Incremental lift

Center of twist

Δ

(a) Incremental loads

Total lift

Normal

Neutral

Reversal

Δ

(b) Total loads

Figure 12.- Effect of control deflection on wing load and moment.

T

θ

Angle of twist, θ

Slope = 1/k

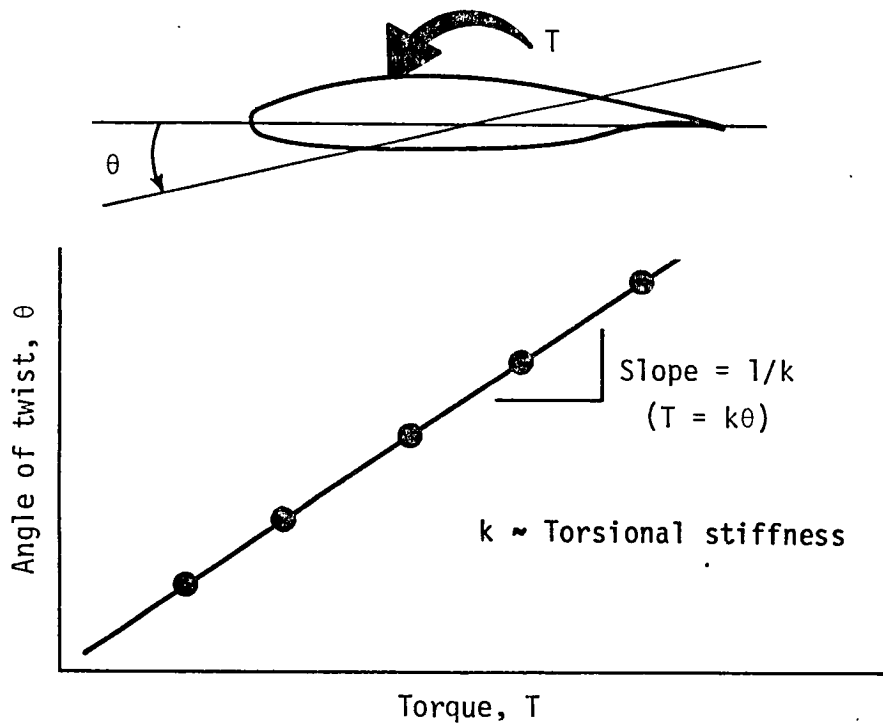$(T = k\theta)$

$k \sim$ Torsional stiffness

Torque, T

Figure 13.- Typical data curve for measuring wing torsional stiffness.

14

Further explanation of aileron reversal is as follows. A deflection Δ of the control surface (positive for trailing edge deflected down) produces an incremental lift at the surface as illustrated in the upper part of figure 12. Because the control is aft of the center of twist, a nose down pitching moment is produced which tends to decrease the wing angle of attack. Reducing the angle of attack causes a reduction in the wing contribution to lift. Normally, the total lift (wing plus control surface aerodynamics) is increased for a positive control deflection. However, if the elastic twist is large enough, the reduction in wing lift exactly equals the additional incremental lift caused by the control deflection. The total lift is unchanged in this case as illustrated in figure 12 by the neutral curve. For this condition no rolling moment is produced and the stick is ineffective. Increasing the aircraft speed will result in a decrease in total lift when the control is deflected and thus produces roll in the direction opposite that intended--that is, the reversal condition. Flight in this condition is possible if the pilot is able to reverse his thinking to push the stick right for a left roll. Recovery is achieved only by slowing down the speed.

During ground tests for aileron reversal evaluation, it is necessary to measure the torsional stiffness of the wing structure. The stiffness can be calculated from measurements of the twist angle made when the structure is loaded incrementally in torsion as illustrated in figure 4. For small twist angles θ at torsional loads T, the data is linear as illustrated in figure 13. The torsional stiffness k is equivalent to the inverse slope of the data.
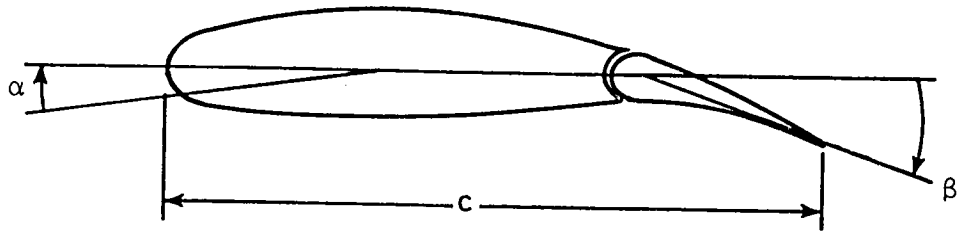
$$q_R = \frac{C_{L_\beta} k}{C_{L_\alpha} C_{MAC_\beta} cS}$$

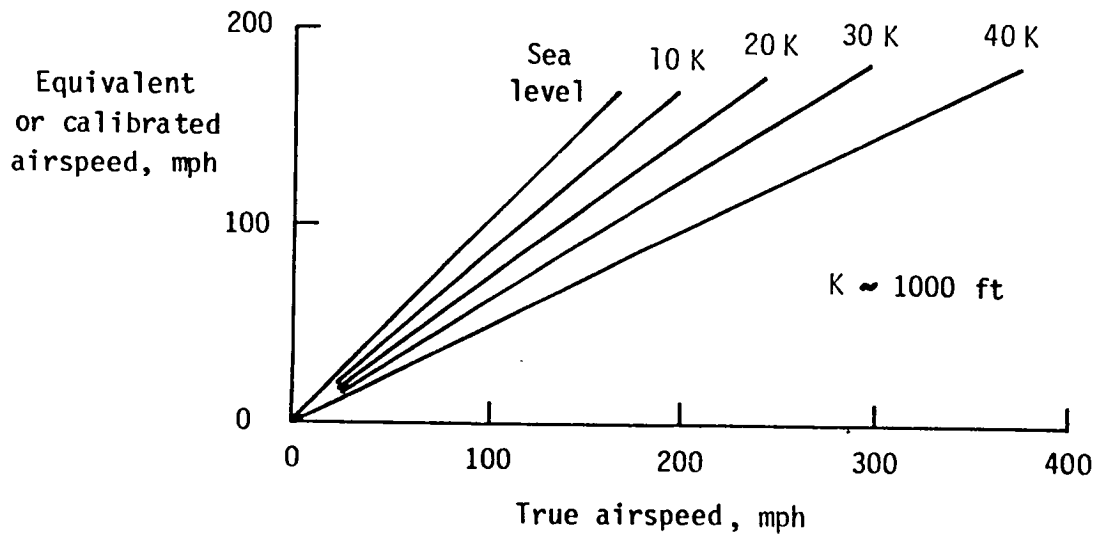Figure 14.- Calculation of control reversal dynamic pressure.

Figure 15.- Relationship between equivalent/calibrated airspeed and true airspeed at various altitudes.

An aileron reversal dynamic pressure[2] can be calculated for a wing shown in figure 14 using the measured wing torsional stiffness k and a few other parameters. The other parameters include the coefficients of lift due to changes in angle of attack C_{L_α} and control deflection C_{L_β}, coefficient of moment about the mean aerodynamic center (MAC) due to control deflection C_{MAC_β}, the wing chord c and the wing area S. (The coefficients may be found in a typical airfoil handbook such as references 8 and 9). The equation for the reversal dynamic pressure q_R is

$$q_R = \frac{-C_{L_\beta} k}{C_{L_\alpha} C_{MAC_\beta} cS}$$

---

[2]A short explanation of dynamic pressure is in order because it is the main parameter that is referenced when discussing aeroelastic problems. Dynamic pressure is defined as one-half the air density times the square of the true airspeed. This is also equal to one-half the air density at sea level times the square of equivalent airspeed. Because calibrated and indicated airspeeds are proportional to equivalent airspeed, dynamic pressure is proportional to the square of calibrated, or indicated, airspeed. Figure 15 shows the relationship between calibrated airspeed and true airspeed for altitudes to 40 000 feet.
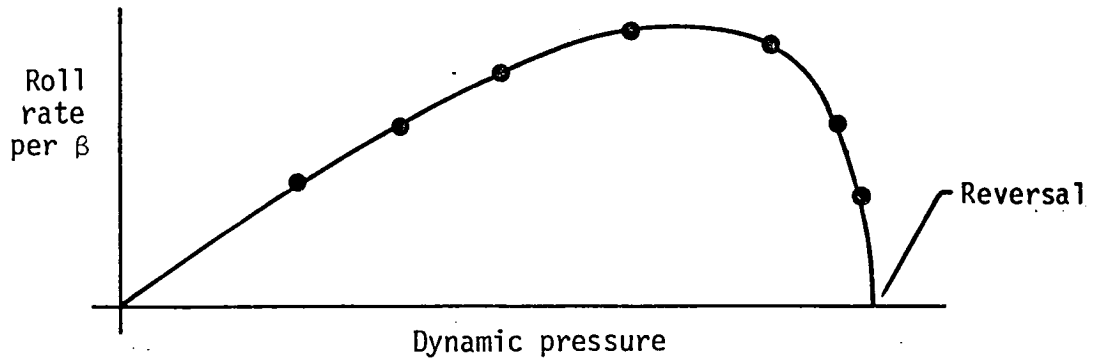
Figure 16.- Typical data measured to determine control reversal.
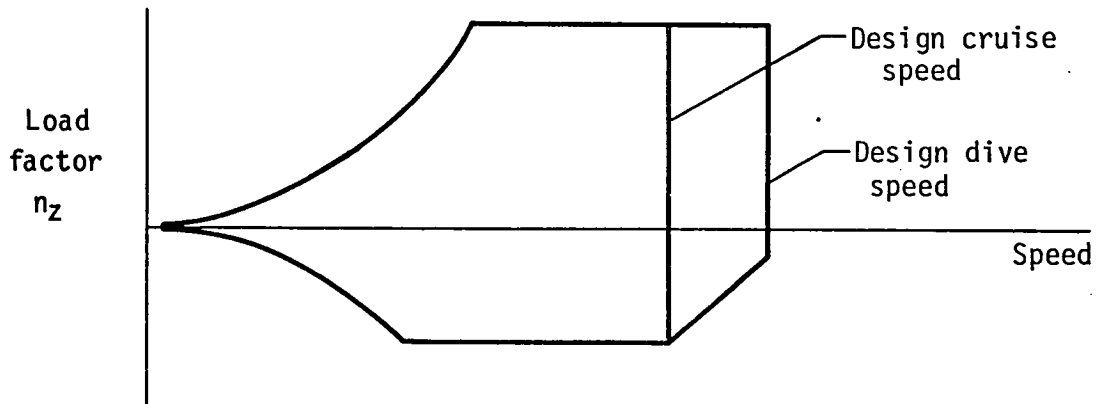

Figure 17.- Typical flight envelope showing relationship between
cruise and dive speeds.

18

During flight test, data may be acquired to predict the dynamic pressure at which aileron reversal may occur. Measurements of roll rate and control surface displacement β at various dynamic pressures may be used to extrapolate to the point of reversal--that is, the condition of zero roll rate per control surface deflection as shown in figure 16. Instrumentation normally used for the measurements include rate gyros, position potentiometer, strain gages, and tape recorders. However, equipment such as a horizon indicator or an inclinometer for measuring roll angle and a stop watch for measuring time may be used to calculate the roll rate. A stop for the control stick may be used to insure that the same control deflection is achieved at each data point.

FAR Part 23 requires that the airplane be free from control reversal throughout the flight envelope shown in figure 17 (simpler version of fig. 8). This may be shown by flight testing the aircraft to dive speeds without experiencing reversal. Or, by analysis, it may be shown that the aircraft is free from reversal up to 40 percent beyond cruise speeds or 20 percent beyond dive speeds, whichever is less.
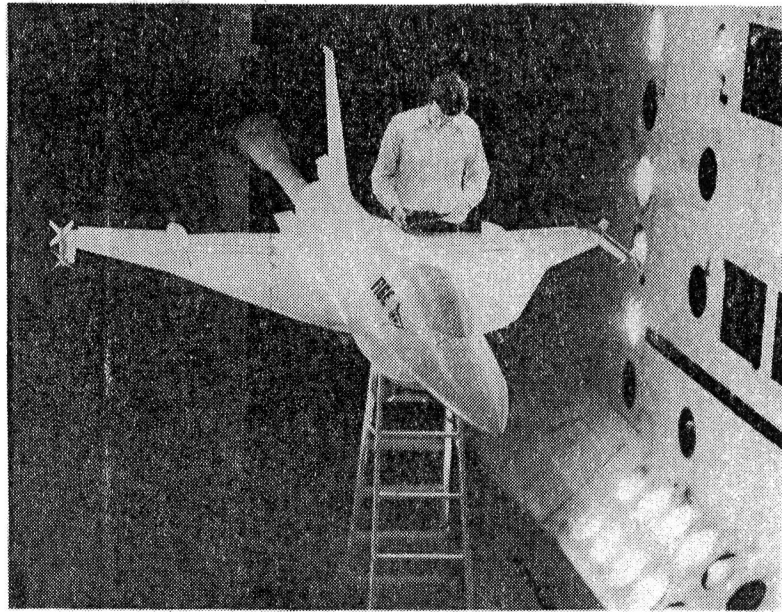
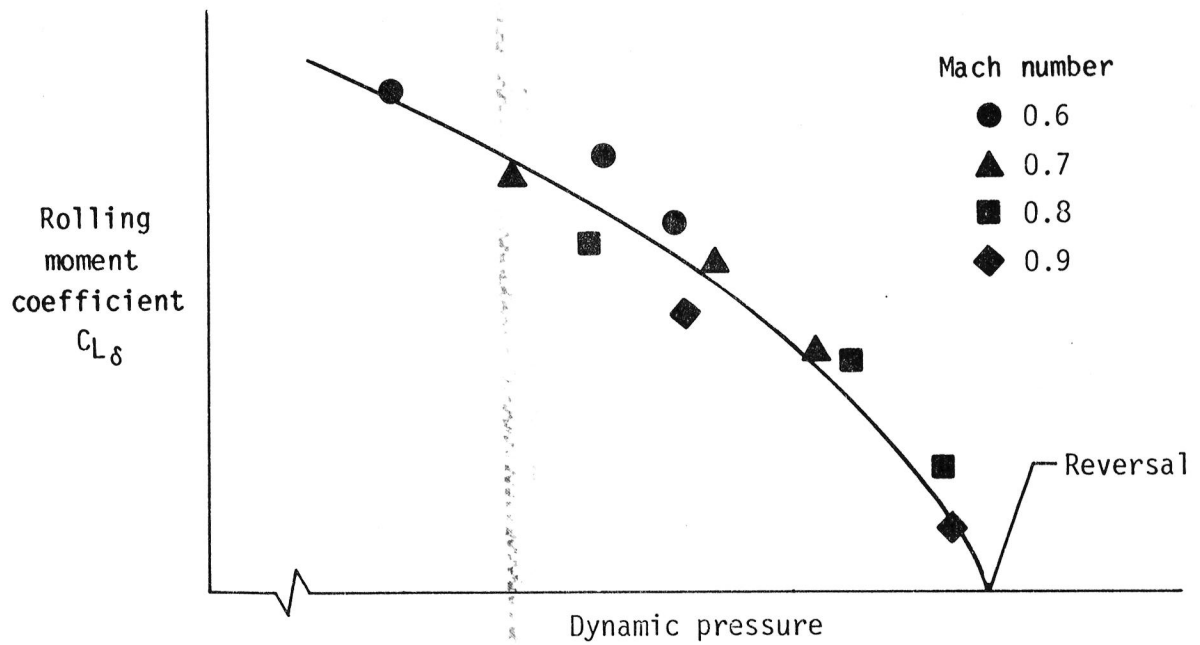Figure 18.- Quarter-scale aeroelastic model mounted in TDT.

Figure 19.- Rolling moment coefficient measurements for predicting
aileron reversal dynamic pressure.

Aileron reversal was measured on a quarter-scale wind-tunnel model of a fighter airplane (ref. 10). The aileron controls were located along the trailing edge at the wing tips of the arrow-wing planform. For the tests the model was supported on a sting in the middle of the NASA Langley Research Center Transonic Dynamics Tunnel (TDT) as shown in figure 18.

Rolling moment coefficients C_{L_δ} were measured using bending moment strain gages positioned at the wing root. The moments were measured for three control deflection angles at each of three values of dynamic pressure at transonic Mach numbers. The data are presented in figure 19 and show that the reversal dynamic pressure may be predicted by extrapolating the data to the zero-rolling-moment value.
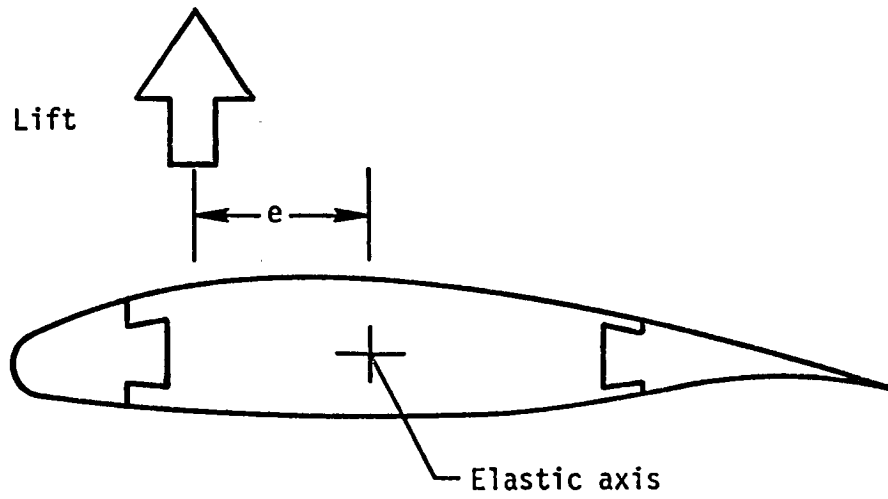
Figure 20.- Typical airfoil section showing relationship between lift and elastic axis.
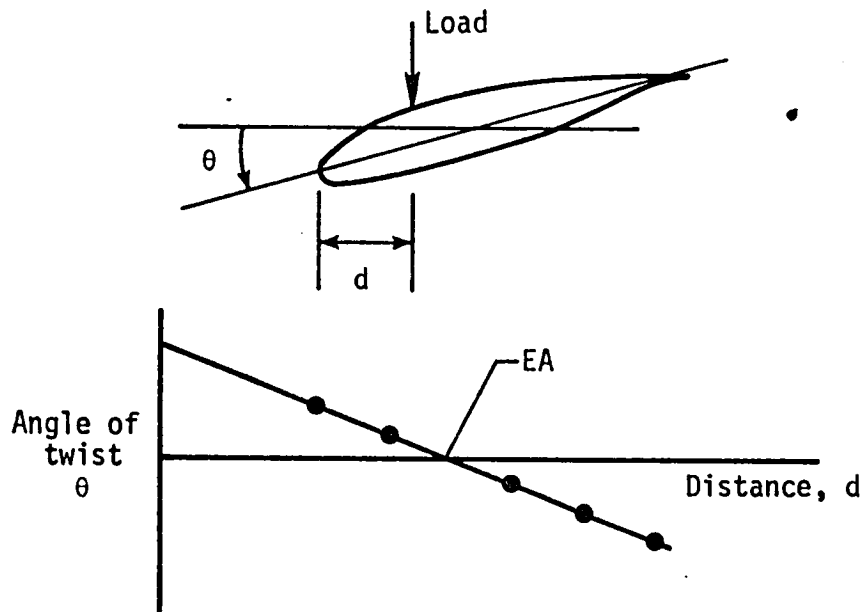

Figure 21.- Measurement of elastic axis (EA) location.

STATIC DIVERGENCE

Static divergence of a lifting surface is a static instability which occurs when the aerodynamic moment on the surface exactly equals the structural elastic restoring moment. Therefore, it is the interaction of aerodynamics and elasticity as previously shown by the shaded area in figure 11. Divergence usually occurs on forward-swept surfaces (ref. 11) but also may occur on unswept or slight aft-swept surfaces. Divergence normally leads to catastropic destruction of the lifting surface when the strength limits of the structure are reached.

Further explanation of divergence is as follows. The product of the resultant lift force illustrated in figure 20 and the distance e from the force to the elastic axis (effective rotation point of the structure) is equal to the aerodynamic torsional moment. For swept wings the relationship e between the lift forces and the local elastic axis locations inboard of the forces determines the twist of the elastic wing. For example, aft-swept wings twist nose down (washout) under load while forward-swept wings twist nose up (washin) under load. When the lift forces act forward of the elastic axis (positive e), divergence can occur. Because forward sweep increases e and, therefore, the aerodynamic moment, forward-swept wings are more susceptible to static divergence than aft-swept wings.

The divergence dynamic pressure may be calculated from measurements made during ground test. It is necessary to measure the torsional stiffness k and the elastic axis location. To measure the torsional stiffness, the angle of twist of the structure is measured during the application of incremental torque loads as previously described. The torsional stiffness is inversely proportional to the slope of the acquired data as previously shown in figure 13.

The elastic axis EA is located by measuring the angle of twist of the structure during the application of a force load at various positions d along the chord. The elastic axis is the location at which an applied force creates pure displacment and no twist θ. An illustration of data acquired during such a test is shown in figure 21.
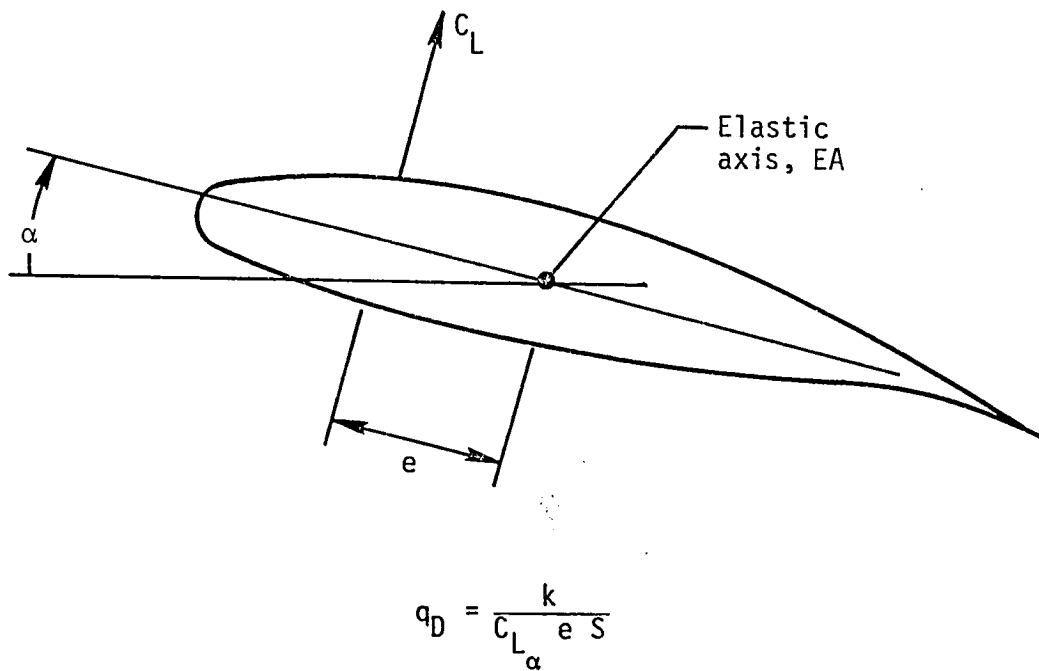
$$q_D = \frac{k}{C_{L_\alpha} e S}$$

Figure 22.- Calculation of divergence dynamic pressure.

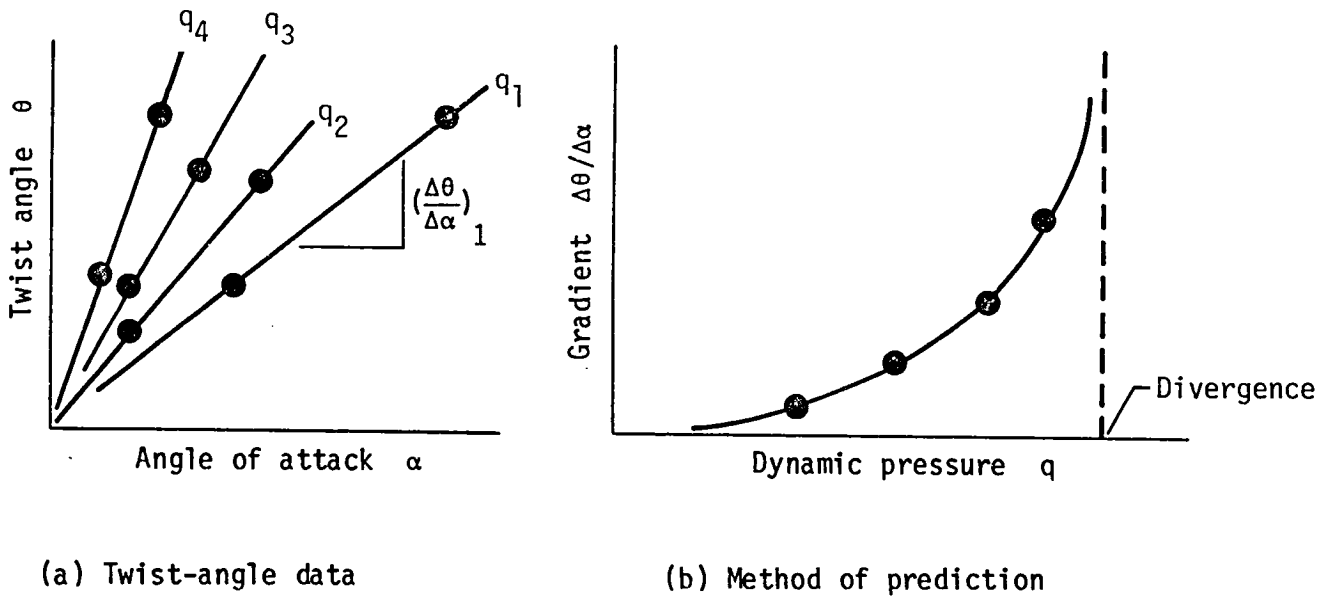(a) Twist-angle data

(b) Method of prediction

Figure 23.- Measurement of divergence dynamic pressure.

The divergence dynamic pressure q_D may be calculated from the following equation

$$q_D = k/(C_{L_\alpha} e S)$$

where k is the torsional stiffness, e is the distance between the elastic axis location and the center of lift (normally assumed to be acting at the quarter-chord), C_{L_α} is the coefficient of lift due to angle of attack, and S is the wing area. This is illustrated in figure 22.

Subcritical response of a lifting surface may be measured in flight to predict the conditions at which divergence will occur. The procedure is as follows. Wing twist angle θ is measured at several angles of attack α for various dynamic pressure conditions q. (The angle of attack may be varied while holding constant altitude and airspeed in a banked turn.) At each dynamic pressure a straight line is fitted through the twist/angle-of-attack data to determine the gradient (or slope) $\Delta\theta/\Delta\alpha$ as shown in figure 23a. The gradients are larger at larger dynamic pressures and become infinite at divergence as shown in figure 23b. Additional methods for predicting the divergence dynamic pressure from measured data are described in reference 11. Instrumentation that is needed include strain gauges calibrated to measure twist angle, angle-of-attack indicator and tape recorder to record the data. Alternately, a camera may be used to record the wing twist for post flight data reduction.

FAR Part 23 requires that the airplane be free from static divergence throughout the flight envelope. This may be shown by flight testing the air-craft at dive speeds without experiencing divergence. Or, by analysis which shows that the aircraft is free from divergence up to 40 percent beyond cruise speed or 20 percent beyond dive speed, whichever is less. These requirements are similar to those presented for aileron reversal. (See fig. 17.)
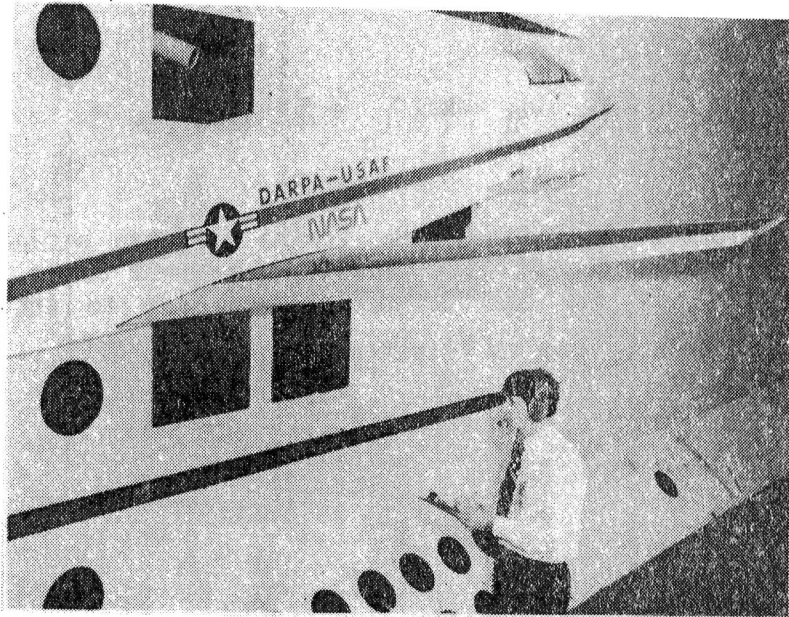
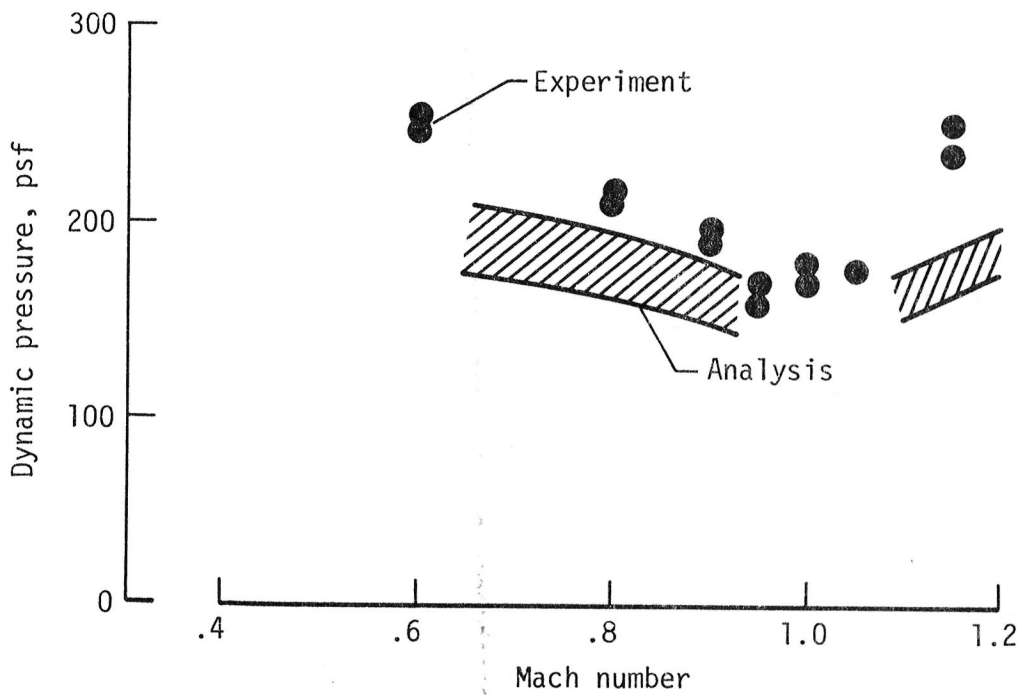Figure 24.- Forward swept wing aeroelastic model mounted in TDT.

Figure 25.- Comparison of experimental and analytical results defining a static divergence boundary.

Static divergence was measured during wind-tunnel tests of the half-scale model of anexperimental aircraft with a forward-swept wing shown in figure 24. (See ref. 12.) The model consisted of an aeroelastically-tailored composite wing, half fuselage, and a closely-coupled canard. The model was mounted to a turntable on the sidewall of the TDT so that angle of attack could be varied to acquire load/angle-of-attack data for various dynamic pressure and Mach number conditions.

Subcritical response techniques were used to predict the divergence dynamic pressure boundary throughout the transonic Mach number range. The experimental predictions are compared in figure 25 with analytical predictions computed using structural finite element modeling techniques and several aerodynamic lifting surface theories. The range of analytical predictions is shown by the shaded area in the figure. The boundary has a minimum divergence dynamic pressure which occurs in the transonic region. (This is similar to typical flutter boundaries. Flutter is discussed in the following section.)
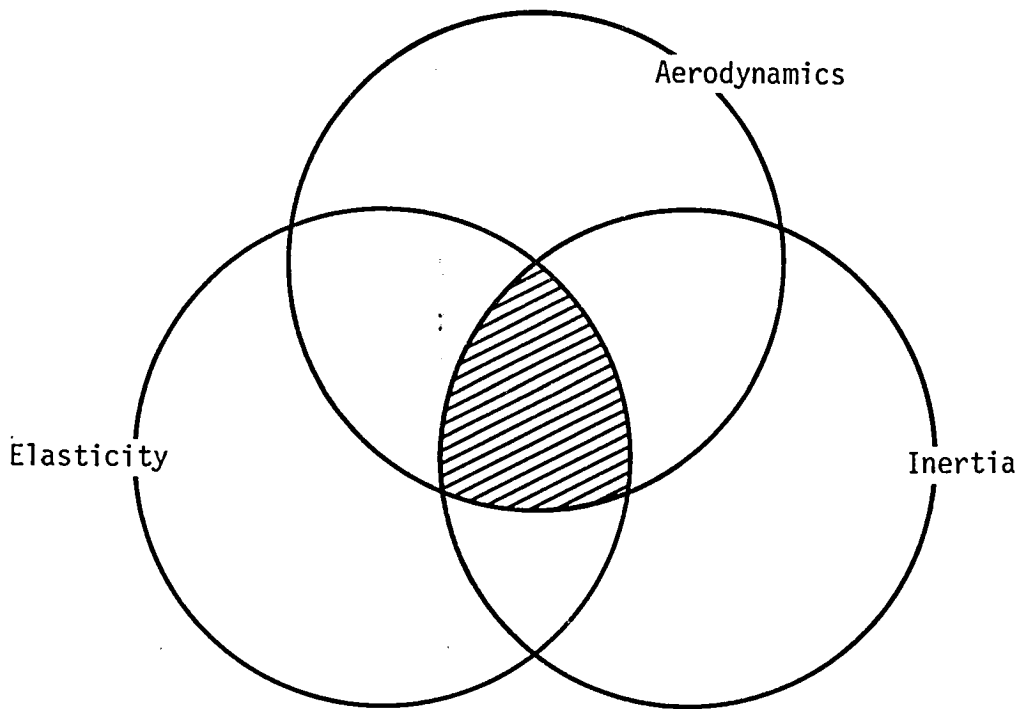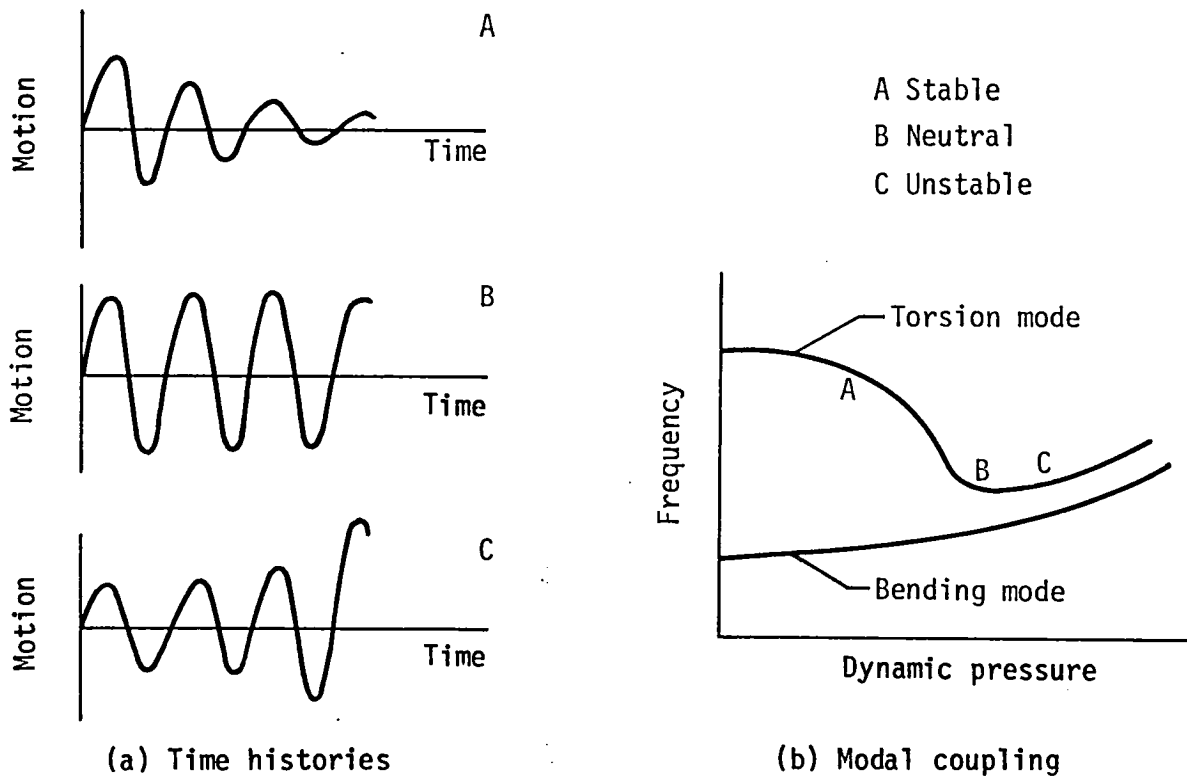
Figure 26.- Interaction diagram for flutter.

A Stable
B Neutral
C Unstable

(a) Time histories

(b) Modal coupling

Figure 27.- Flutter stability of a typical wing structure.

FLUTTER

Flutter is a dynamic instability which occurs when the aerodynamic, inertia, and elastic forces couple to cause a self-excited motion of a lifting surface. The flutter motion is sinusoidal and may be either constant or divergent in amplitude. Flutter, particularly that with divergent motions, may cause catastrophic destruction. The interaction of the three ingredients to flutter is shown by the shaded area in figure 26.

Further explanation of flutter is as follows. Time histories of typical structural responses are shown for three dynamic pressure conditions in figure 27a. The time history for condition A shows motion that is damped and stable--that is, after a disturbance the amplitude decreases with time. The time history for condition B shows constant-amplitude motion that indicates neutral stability. The time history for condition C shows a divergent or unstable condition--that is, the amplitude increases with time. Both the neutral and unstable conditions represent flutter conditions.

In classical wing flutter the torsion mode coalesces (or couples) with the bending mode. The modal frequencies change with dynamic pressure as shown in figure 27b. As the flutter dynamic pressure is approached the torsion frequency usually decreases substantially, and the bending frequency increases slightly. At flutter the two modes couple, and the wing oscillates at a single frequency. Typical conditions at which the time histories (A, B, and C) occur are indicated in the figure. Additional information is given in reference 13.

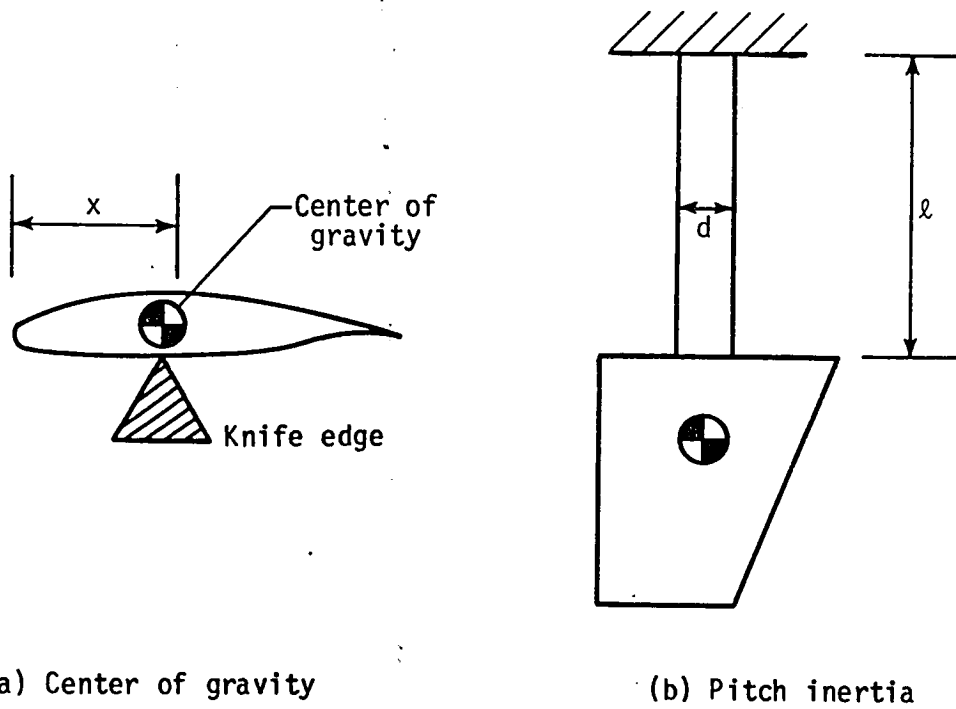(a) Center of gravity   (b) Pitch inertia

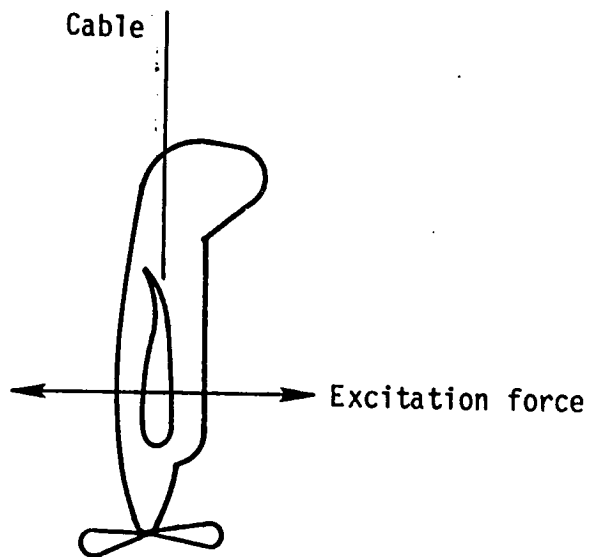Figure 28.- Measurement of mass properties of wing.

Figure 29.- Airplane support for ground vibration test.

A simple flutter analysis of a lifting surface may be performed using strip theory aerodynamics and structural data. The aerodynamic parameters such as lift-curve slope and center of pressure location may be found in a typical aerodynamic handbook (ref. 8). The structural data, which includes the elastic axis location, mass properties, and vibration frequencies, may be acquired during ground test described as follows.

Measurement of the elastic axis location is performed as previously described. The angle of twist of the structure is measured for various load applications along the surface chord. Recall that the elastic axis is the load location which produces deflection but no angle of twist. (See fig. 21.)

The following mass properties may be measured in ground test: weight, center of gravity, and inertia. The weight of the surface may simply be measured with scales. The center of gravity CG may be located in terms of a distance x from the leading edge by balancing the surface on a "knife edge." The "knife edge" is moved until the point of balance is obtained as shown in figure 28a. The pitch inertia of the surface may be measured using a bifilar pendulum--that is, a pendulum that has two filaments (or cables) as shown in figure 28b. The cables are positioned symmetrically about the CG a distance d apart. The length ℓ of the cables should be at least ten time longer than d to maintain good accuracy. The period T (or time) that the surface moves through a complete cycle of oscillation may be measured with a stop watch. (The surface is displaced in twist on the cables about 30 degrees and released. Timing is begun as the surface passes a reference point and continues until the surface passes the reference point several times, usually ten or more. The period, or the average time for one cycle, is computed by dividing the total time by the total number of cycles). The pitch inertia may be computed using the following equation

$$I = 2.444 \ W \ d^2 \ T^2/\ell, \ lb\text{-}in^2$$

where the weight W is in units of pounds, lengths are in inches, and the period is in seconds.

Ground vibration testing which is performed to measure the natural vibration characteristics, particularly the resonant frequencies, of the structure, is described as follows. The structure to be tested must be supported so that the support mechanism does not influence the vibration characteristics of the structure alone. A good rule of thumb to follow is that the frequencies of the support modes should be on the order of ten percent of the frequency of the first structural mode. Often this can be achieved by simply deflating the tires of the aircraft. However, it may be necessary to suspend the aircraft on soft springs. The structure may also be supported as a pendulum with a low pendulum frequency. In this case the mode excitation force would be applied normal to the pendulum cable as shown in figure 29.

(a) Electromagnetic shaker
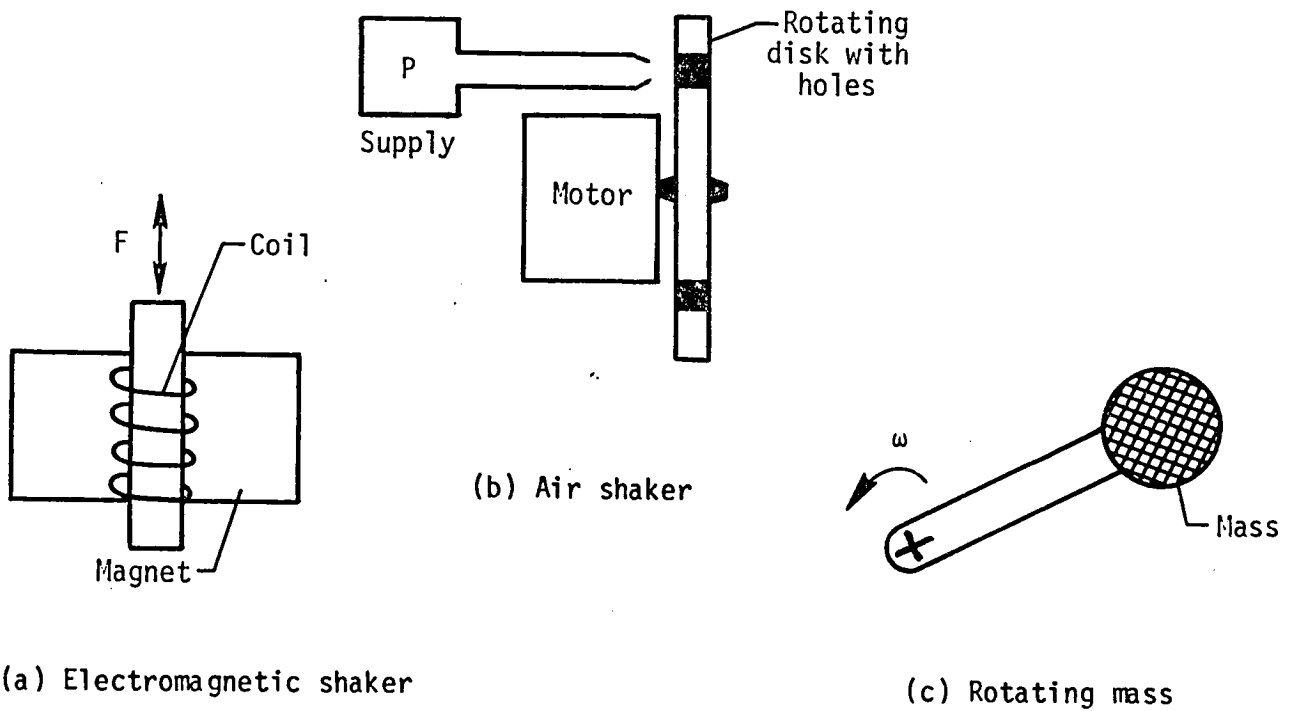
(b) Air shaker

(c) Rotating mass

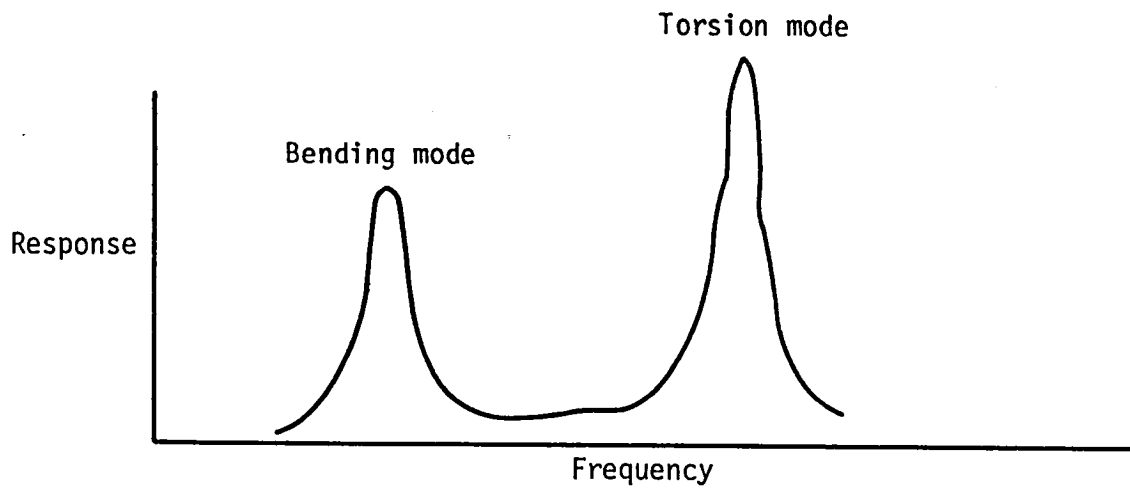Figure 30.- Typical devices for exciting a structure.

Figure 31.- Typical frequency response of wing structure.

Equipment that may be used to sinusoidally excite the structure include electromagnetic shakers, pulsating air jets, and rotating masses. An electromagnetic shaker as illustrated in figure 30a may be used with an oscillator to drive it. A pulsating air jet device as illustrated in figure 30b may be easily fabricated using an air compressor to supply air which is directed toward the wing surface and deflected by a rotating disk with holes in it. The disk is driven by a variable speed motor. The air-jet device is particularly useful for lightweight structures because no additional mass is attached to the structure. A rotating-mass device as shown in figure 30c is the easiest shaker to fabricate. An eccentric weight is rotated using a variable speed motor. The vibration force is directly portional to the eccentricity e, the mass of the weight, and the square of the rotation frequency ω. It is important that neither the weight nor location of the device influence the frequencies of the structure.

Excitation of structures at their resonant, or natural, frequencies will cause the structural response of the structures to increase. The natural frequencies may be measured by exciting the structure with shaker equipment while slowly varying the excitation frequency and monitoring the structural response. The response may be monitored with an analyzer, strip chart, or, in some cases, visually. The frequencies at which the response is a maximum (see fig. 31) for constant shaker force are the natural frequencies of the structure. The value of the frequency may be determined with an oscilloscope, a strobe light, or, for frequencies less than three Hertz, a stop watch. It is also possible to use a timing light and tachometer attached to a running engine to measure the frequency of vibration of the structure.

Air density ρ

Air volume πb²

b

Mass ratio $\mu = \dfrac{w}{\pi \rho b^2}$

Wing weight
per unit length w

Figure 32.- Mass ratio calculation.

Data point

1   2   3

Flight no.

4   5   6

7   8   9

Altitude

Airspeed, IAS
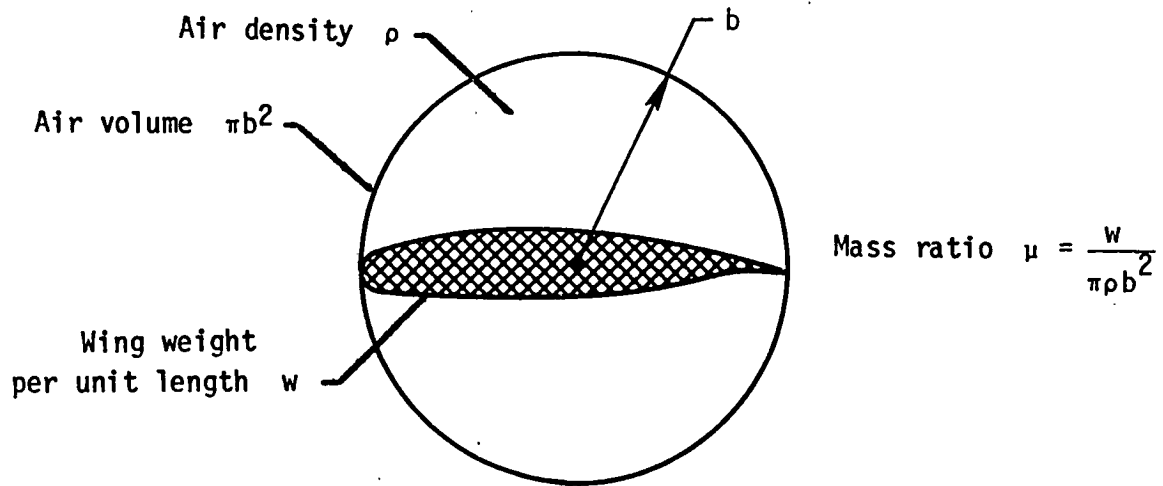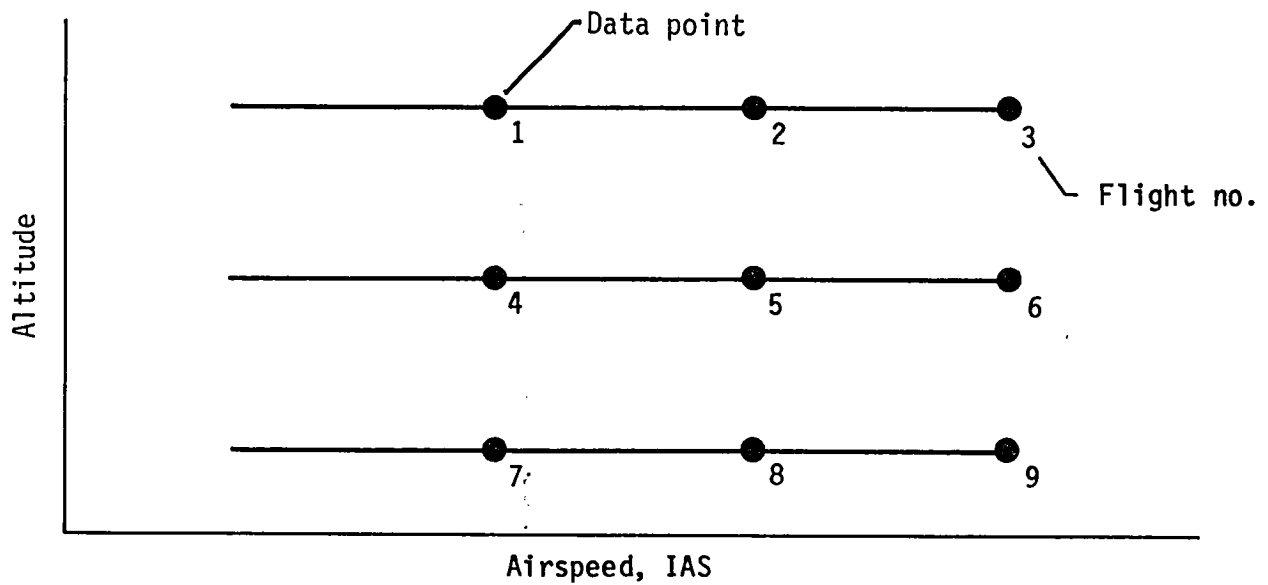
Figure 33.- Typical flight plan for flutter testing.

A rule of thumb to follow for approximating the flutter speed of a lifting surface with a conventional planform (zero to moderate aft sweep angles) uses a parameter called the flutter speed index FSI which is defined by the following equation:

$$FSI = V/(b\omega\sqrt{\mu})$$

where V is the flutter speed (feet per second), b is the length (feet) of the semichord at the three-quarter span, ω is the natural frequency (radians per second) of the torsion mode, and μ is the ratio of the wing weight to the weight of the volume of air in a frustrum of a cone enclosing the wing. For a constant chord wing μ is simply the wing weight per unit length ω divided by π, the air density ρ, and the square of the semichord as illustrated in figure 32. The rule of thumb is that FSI is approximately equal to one-half at all altitudes. Thus, substituting the values of the parameters, including the air density at a particular altitude, into the equation for FSI equal to 0.5, the approximate flutter speed may be calculated. See reference 14 for additional information.

Flight testing for flutter (ref. 15) requires a flight plan to insure maximum safety. An example plan is shown in figure 33. The aircraft is tested at several velocities at each of several altitudes. Response of the aircraft to excitation may be monitored visually from the cockpit or from a chase plane, electronically using strain gages or accelerometers, or photographically using a movie camera mounted on the aircraft.
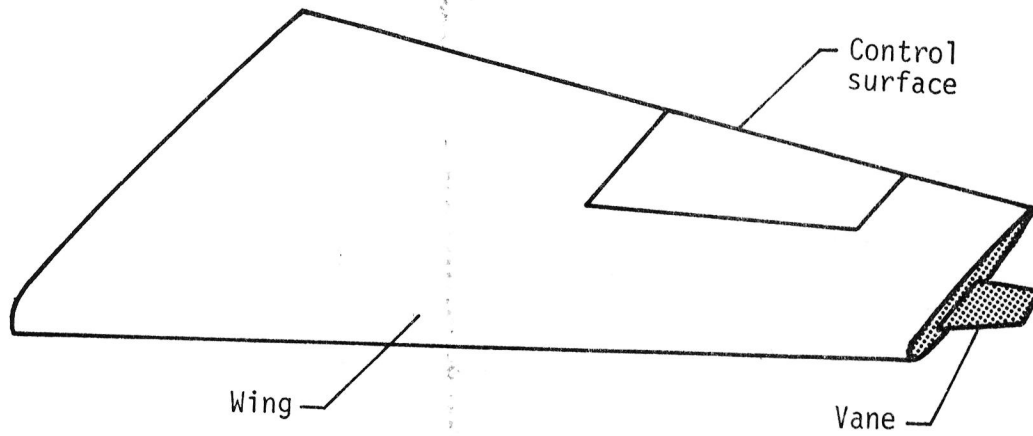
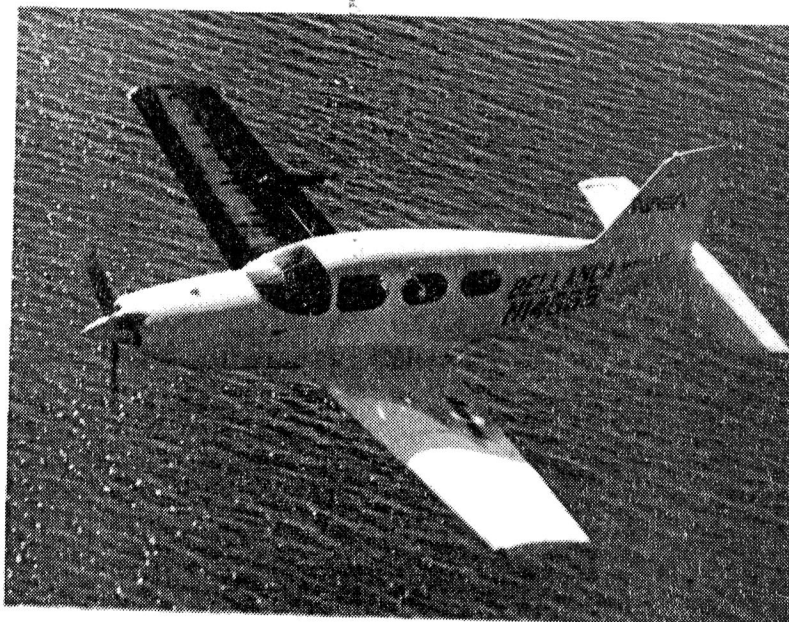Figure 34.- Aerodynamic vane for structural mode excitation during flutter testing.

Figure 35.- Experimental aircraft for conducting laminar flow studies.

During flight tests the aircraft structure may be excited using a variety of methods. For a broad range of frequencies random ambients such as atmospheric turbulence or engine vibrations may be used in some cases. However, the level of excitation is not controllable and also is difficult to measure. For low frequencies (less than ten Hertz) pilot induced impulses from the controls may be used. For higher frequencies the excitations may be input to the structure through inertia or electromagnetic shakers attached to wing structure or control linkages. Another device that is often used is an aerodynamic vane attached to the wing tip as shown in figure 34 and driven by an electric motor or hydraulic actuator.

FAR Part 23 requires that the airplane be free from flutter throughout the flight envelope. This may be shown by flight testing the aircraft to dive speed without experiencing flutter. Or, by analysis, it may be shown that the aircraft is free from flutter up to 40 percent beyond cruise speed or 20 percent beyond dive speed, whichever is less. These requirements are similar to those presented for aileron reversal and static divergence. (See fig. 17.)

Ground test and flight test (ref. 16) of the experimental aircraft shown in figure 35 were conducted at Langley Research Center to determine the flutter speed of the horizontal tail so that laminar flow studies could be conducted on the aircraft wing. Ground vibration tests were conducted to measure the natural frequencies, mode shapes, generalized masses, and structural damping. The results were used in a flutter analysis which included lifting surface unsteady aerodynamics. The horizontal tail was instrumented with two accelerometers and then flight tested to record the tail response to random ambient turbulence.
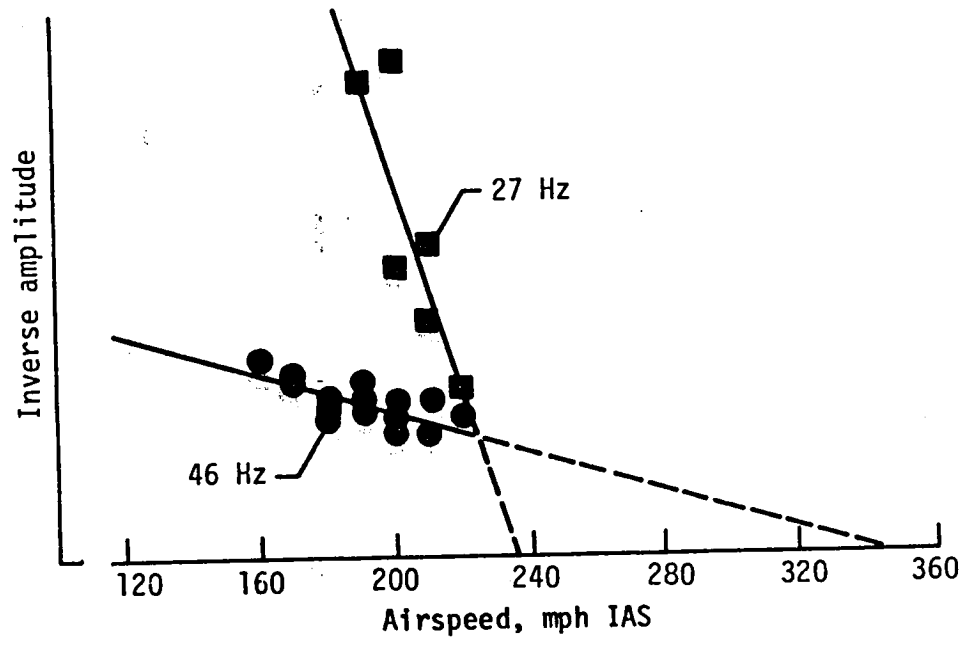
Figure 36.- Inverse amplitude data for predicting horizontal tail flutter.

Subcritical response techniques (ref. 17) were used on the recorded data to predict the flutter onset speed of the horizontal tail. One such technique is called the peak hold method which uses measured peak rms (root mean square) response at incremental frequences throughout the frequency range of interest to predict flutter. As a flutter condition is approached, the peak increases in amplitude until, at flutter, it theoretically becomes infinite; or, in other words, at flutter, the inverse amplitude is zero. Results of data anlaysis using the peak hold method are shown in figure 36 for two different possible flutter modes. A 27 Hz mode is predicted to flutter at an airspeed of 235 mph. This speed is lower than that predicted for the 46 Hz mode. The aircraft speed was therefore limited to 205 mph to allow a 15 percent margin in speed for overshoots during the laminar flow tests.

CONCLUDING REMARKS

Ground test and flight test methods have been described that may be used to highlight potential structural problems that occur on aircraft. The structural problems described include static strength failure, aileron reversal, static divergence, and flutter. An example of each of the problems was discussed to illustrate how the data acquired during the tests may be used to predict the occurance of the structural problem. Furthermore, the requirements that are set forth in the Federal Aviation Regulations to insure that each problem does not exist within the flight envelope were discussed.

REFERENCES

1. Bisplinghoff, R. L.; Ashley, H.; and Halfman, R. L.: Aeroelasticity. Second edition. Addison-Wesley Publishing Company, Inc., 1957.

2. NATO Advisory Group for Aerospace Research and Development (AGARD): Manual on Aeroelasticity, volumes I-VI. Technical Editing and Reproduction Ltd., 1968.

3. Fung, Y. C.: An Introduction to the Theory of Aeroelasticity. Dover Publications, Inc., 1969.

4. Timoshenko, S.; and Young, D. H.: Strength of Materials. Fourth Edition. D. Van Nostrand Company, Inc., 1962.

5. Federal Aviation Administration: Federal Aviation Regulations, Part 23, Airworthiness Standards - Normal, Utility, and Aerobatic Category Airplanes, 1974.

6. Murrow, H. N.; and Eckstrom, C. V.: Drones for Aerodynamic and Structural Testing (DAST) - A Status Report. Journal of Aircraft, vol. 16, no. 8, Aug. 79, pp. 521-526.

7. Eckstrom, C. V.: Loads Calibration of Strain Gage Bridges on the DAST Project Aeroelatic Research Wing (ARW-1). NASA TM 81889, 1980.

8. Abbott, Ira H.; and Von Doenhoff, Albert E.: Theory of Wing Sections. Dover Publications, Inc., 1959.

9. Dommasch, D. O.; Sherby, S. S.; and Connolly, T. F.: Airplane Aerodynamics. Third edition. Pitman Publishing Corporation, 1961.

10. Bensinger, C. T.: F-16E 1/4 Scale Flutter Model First Test (September 1981). General Dynamics/Fort Worth Division Report No. 400PR032, 1981.

11. Ricketts, R. H.; and Doggett, R. V., Jr.: Wind-Tunnel Experiments on Divergence of Forward-Swept Wings. NASA TP 1685, 1980.

12. Hertz, T. J.; Shirk, M. H.; Ricketts, R. H.; and Weisshaar, T. A.: On the Track of Practical Forward-Swept Wings. Astronautics and Aeronautics vol. 20, no. 1, Jan. 1982, pp. 40-52.

13. Scanlan, R. H.; and Rosenbaum, R.: Aircraft Vibration and Flutter. Dover Publications, Inc., 1968.

14. Harris, G.: Flutter Criteria for Preliminary Design. Vought Aeronautics Report 2-53450/3R-467, 1963.

15. Kordes, E. E., Chairman: Flutter Testing Techniques. Proceedings of a conference held at Dryden Flight Research Center, in Edwards, CA, Oct. 9-10, 1975. NASA SP-415, 1975.

16. Ricketts, R. H.; Cazier, F. W., Jr.; and Farmer, M. G.: Flutter Clearance of the Horizontal Tail of the Skyrocket II Airplane. NASA TM 84528, 1982.

17. Ruhlin, C. L.; Watson, J. J.; Ricketts, R. H.; and Doggett, R. V., Jr.: Evaluation of Four Subcritical Response Methods for On-line Prediction of Flutter Onset in Wind-Tunnel Tests. NASA TM-83278, 1982. Presented at AIAA/ASME/ASCE/AHS 23rd Structures, Structural Dynamics, and Materials Conference, New Orleans, LA, May 10-12, 1982. AIAA Paper No. 82-0644, May 1982. (Also available as NASA TM 83278.)

1. Report No. NASA TM-84606	2. Government Accession No.	3. Recipient's Catalog No.
4. Title and Subtitle Structural Testing for Static Failure, Flutter and Other Scary Things		5. Report Date January 1983
		6. Performing Organization Code 505-33-43-07
7. Author(s) Rodney H. Ricketts		8. Performing Organization Report No.
		10. Work Unit No.
9. Performing Organization Name and Address NASA/Langley Research Center Hampton, VA 23665		
		11. Contract or Grant No.
		13. Type of Report and Period Covered Technical Memorandum
12. Sponsoring Agency Name and Address National Aeronautics and Space Administration Washington, DC 20546		
		14. Sponsoring Agency Code

15. Supplementary Notes

Technical paper presented at Annual Convention of Experimental Aircraft Association, Oshkosh, WI, August 1982.

16. Abstract

Ground test and flight test methods are described that may be used to highlight potential structural problems that occur on aircraft. Primary interest is focused on light-weight general aviation airplanes. The structural problems described include static strength failure, aileron reversal, static divergence, and flutter. An example of each of the problems is discussed to illustrate how the data acquired during the tests may be used to predict the occurrence of the structural problem. While this report gives some rules of thumb for the prediction of structural problems, it is not intended to be used explicitly as a structural analysis handbook. However, many such handbooks are included in the reference list.

17. Key Words (Suggested by Author(s)) Ground Test Flutter Flight Test Static Strength Failure Aileron Reversal Static Divergence	18. Distribution Statement Unclassified - Unlimited Subject Category 39

19. Security Classif. (of this report) Unclassified	20. Security Classif. (of this page) Unclassified	21. No. of Pages 42	22. Price A03